IIAI Open Conference Publication Series
IIAI Letters on Business and Decision Science
Vol. 004, LBDS246
DOI: https://doi.org/10.52731/lbds.v004.246

Proposal of an SEIR Model Considering Inter-group Human Movement among Large Scale of Groups

Hiroyoshi Matsumoto [*], Yusuke Yamauchi [*],
Shimpei Matsumoto [*]

Abstract

This study proposes an epidemic model using person trips and treats the SEIR model as the research model, which extends the SIR model. The study analyzes the actual spread of the Omicron strain of the coronavirus, which occurred throughout Japan around the beginning of the fiscal year 2022. After obtaining the epidemic model based on the SEIR model, the study divides a single epidemic area into four groups to reproduce diverse infections through person trips. Using the records of the number of infected individuals and commuters in Saitama, Tokyo, Kanagawa, and Chiba prefectures from January to April 2022, the study estimates the parameter values of infection rate, recovery rate, and mobility rate. The study discusses epidemic control by applying the estimated parameter values and compares the newly infected data of Saitama, Tokyo, Kanagawa, and Chiba prefectures used in parameter estimation with the infection data to evaluate the utility of the model. Additionally, the study examines the simulation results by varying the mobility rates through several patterns.

Keywords: SEIR model, Epidemic model, Person trip, Covid_19,

1 Introduction

The COVID-19 pandemic has wreaked havoc globally, including in Japan, with a total of 33,803,572 infections and 74,694 deaths recorded as of December 31, 2023. As of January 2024, although the momentum of infections has diminished compared to the early stages of the outbreak, measures still need to be taken.

The SIR (Susceptible-Infectious-Recovered) model, formulated by Kermack and McKendrick in 1927, represents the short-term epidemic process of infectious diseases through classical model equations (1). The SIR model assumes the absence of immunity to the novel infectious disease, no population movement between external cities, population density with contact with an unspecified large number of people, and a rapid and short-term outbreak like the plague. The name is derived from the initials of the susceptible individuals (S), infected individuals (I), and recovered or removed individuals (R). On the other hand, the SEIR model extends the SIR model by considering exposed individuals (E) due to the infectious disease (2). During the Ebola virus outbreak in West Africa from 2014 to 2015, an extension of the SIR model was applied to epidemic analysis to suppress infection spread (3).

[*] Hiroshima Institute of Technology, Hiroshima, Japan

The differential equations for each model are as follows:

$$\frac{dS}{dt}(t) = -\frac{\alpha S(t)I(t)}{N}$$

$$\frac{dI}{dt}(t) = \frac{\alpha S(t)I(t)}{N} - \beta I(t)$$

$$\frac{dR}{dt}(t) = \beta I(t)$$

Figure 1: Differential equations of the SIR model

$$\frac{dS}{dt}(t) = -\frac{\alpha S(t)I(t)}{N}$$

$$\frac{dE}{dt}(t) = \frac{\alpha S(t)I(t)}{N} - \varepsilon E(t)$$

$$\frac{dI}{dt}(t) = \varepsilon E(t) - \beta I(t)$$

$$\frac{dR}{dt}(t) = \beta I(t)$$

Figure 2: Differential equations of the SEIR model

The investigation of human mobility within specific regions, such as between cities, is referred to as a "person trip survey." Previous research (3) employed this concept to conduct numerical calculations targeting influenza. The research examined multiple intercity movements from the perspective of a person trip survey, determining the next-generation matrix and calculating the basic reproduction number and city-specific basic reproduction numbers.

However, considering that the previous research primarily focused on influenza, there may be some differences in the context compared to the current focus on COVID-19. The SIR model assumes that susceptible individuals (S) are infected by infectious individuals (I). However, in reality, infectious individuals (I) are isolated upon being diagnosed positive, making it unlikely for them to directly impact susceptible individuals (S). Therefore, this study assumes that the impact on susceptible individuals (S) is exerted by exposed individuals (E). Additionally, this study assumes that human mobility only occurs between the four groups to examine how human movement affects the spread of infection.

Many studies employing the SIR model assume a constant contact rate, denoted as α. However, in human societies engaged in social activities, the assumption of a constant contact rate at all times does not align with reality. Thus, this study constructs a SEIR model incorporating population movement only during daytime hours. The study determines parameters such as the infection rate and initial values based on real data from Saitama, Tokyo, Kanagawa, and Chiba prefectures, and compares and analyzes them against real-world trends. Furthermore, the study investigates how the number of new infections changes due to the movement of individuals among four groups with different infection rates α, and discusses what measures may be effective in preventing the spread of infectious diseases based on the results.

2 Concept

This section provides a detailed explanation of the SEIR model used in the study, incorporating person trips and variations in contact rates due to diurnal human mobility. The equations derived in this section form the basis for the numerical computations and simulations performed in the study to analyze the spread of the COVID-19 Omicron variant in Japan.

2.1 Prerequisite

The period referenced in devising this model coincides with the period of epidemic prevention measures, presuming minimal outings beyond necessary errands such as commuting or attending school. Thus, considerations exclude travelers from abroad or other prefectures. Parameters such as re-infection or demographic changes like births and deaths are not encompassed due to the utilization of the SEIR model. Effects such as immune enhancement from vaccination or prior infection are not factored in. Furthermore, asymptomatic carriers, being difficult to observe, and their potential impact on non-carriers remain uncertain and hence are not considered.

All initial values utilized in this model are sourced exclusively from national or local government data.

The authors deliberate on the impact of human mobility on infection spread within this model.

2.2 Epidemic Model

This section formulates the extension of the SIR model using person trips. The Kermack-Mckendrick SIR model serves as the foundation of this epidemic model. The SIR model categorizes the population of an epidemic region into three compartments: "susceptible," "infectious," and "recovered." The SIR model employs a system of coupled differential equations to represent transitions between these compartments. S, I, and R represent susceptible, infectious, and recovered individuals, respectively, where S denotes the number of susceptible individuals, I denotes the number of infectious individuals, and R denotes the number of recovered individuals. The difference between S and I is proportional to the number of susceptible individuals in contact with infectious individuals. Additionally, the difference

between I and R is proportional to the number of infectious individuals. Therefore, the differences among S, I, and R are expressed by the following equations.

To resolve these issues using the SEIR model, the epidemic area is partitioned into four groups, defining the susceptible, infected, and recovered individuals of Group 1 as S1, E1, I1, R1.

Furthermore, this framework accommodates different infectious diseases per person trip. α_1 denotes the infection rate of Group 1, β_1 signifies the recovery rate of Group 1, N_1 represents the total population in that group (S1 + E1 + I1 + R1), and T12 denotes the migration rate from Group 1 to Group 2.

Let λ represent the number of new infections during the daytime in Group 1. The number of susceptible individuals in Group 1 during the daytime is denoted as $S_1^d(t)\frac{T_{1,1}}{N_1^d}$. The count of infected individuals in Group 1 during the daytime is given by $S_1^d(t)\frac{T_{1,1}}{N_1^d}$, obtained from the migration rate from Group 1 to Group 1, denoted as T1.1, and the daytime population N_1 of Group 1. The number of latent individuals moving to Group 1 during the daytime is provided for Groups 1 through 4, denoted as$T_{1\sim 4,1}E_{1\sim 4}$ and the total number of latent individuals moving from all groups to Group 1 is given as $\left(T_{1,1}E_1(t) + T_{2,1}E_2(t) + T_{3,1}E_3(t) + T_{4,1}E_4(t)\right)$. Denoting the infection rate of Group 1 as α1, the expression for susceptible individuals in Group 1 becoming infected and becoming new infections is $S_1^d(t)\frac{T_{1,1}}{N_1^d}\alpha_1\left(T_{1,1}E_1(t) + T_{2,1}E_2(t) + T_{3,1}E_3(t) + T_{4,1}E_4(t)\right)$.

By substituting the above expressions from Groups 1 through 4, the following equations are derived.

$$\begin{aligned}\lambda_1^d = {} & S_1^d(t)\frac{T_{1.1}}{N_1^d}\alpha_1\left(T_{1,1}E_1(t) + T_{2,1}E_2(t) + T_{3,1}E_3(t) + T_{4,1}E_4(t)\right) \\ & + S_1^d(t)\frac{T_{1,2}}{N_2^d}\alpha_2\left(T_{1,2}E_1(t) + T_{2,2}E_2(t) + T_{3,2}E_3(t) + T_{4,2}E_4(t)\right) \\ & + S_1^d(t)\frac{T_{1,3}}{N_3^d}\alpha_3\left(T_{1,3}E_1(t) + T_{2,3}E_2(t) + T_{3,3}E_3(t) + T_{4,3}E_4(t)\right) \\ & + S_1^d(t)\frac{T_{1,4}}{N_4^d}\alpha_4\left(T_{1,4}E_1(t) + T_{2,4}E_2(t) + T_{3,4}E_3(t) + T_{4,4}E_4(t)\right) \end{aligned} \quad (1)$$

Let λ_1^n denote the number of new infections during the nighttime. Assuming no inter-group movement during the nighttime, the susceptible individuals present at night are denoted as

S_1^n. They are determined by the infection rate α_1, the latent individuals E1, the total nighttime population N1 of Group 1, and the secondary infection rate within household contacts h(4).

The secondary infection rate within households is referenced from data provided by the National Institute of Infectious Diseases. The institute calculates the secondary infection rate within households (PCR positivity rate among close contacts) based on the basic attributes and contact history of infected individuals and close contacts within households (including non-family members).

The following equation calculates the number of new infections during the nighttime in Group 1.

$$\lambda_1^n = \alpha_1 h \frac{S_1^n(t)}{N_1^n} E_1(t) \quad (2)$$

To determine the number of new infections λ_1 in Group 1, the following equation is derived by calculating the average of the sum of the daytime new infections λ_1^d in Group 1 and the nighttime new infections λ_1^n in Group 1.

$$\lambda_1(t) = \frac{1}{2}(\lambda_1^d + \lambda_1^n) \quad (3)$$

Let S_1 represent the susceptible individuals in Group 1, and as susceptible individuals in Group 1 transition to newly infected individuals, the number of susceptible individuals decreases, denoted as $-\lambda_1(t)$.

$$\frac{dS_1}{dt}(t) = -\lambda_1(t) \quad (4)$$

The latent period of the COVID-19 Omicron variant, the subject of this study, has been disclosed to be approximately 3 days, according to the data published by the National Institute of Infectious Diseases (5). Therefore, it is assumed that individuals who are susceptible in this study will develop symptoms precisely 3 days after being infected by latent individuals. Consequently, the number of latent individuals, denoted as E_1 (t) in Group 1, is the sum of individuals in latent period 1 ($E_{1.1}$ (t)), latent period 2 ($E_{1.2}$ (t)), and latent period 3 ($E_{1.3}$ (t)). The following is a list of

$$E_1(t) = E_{1.1}(t) + E_{1.2}(t) + E_{1.3}(t) \quad (5)$$

Let $E_{1.1}$ denote individuals in Group 1 on the first day of the latent period. There is no data available on latent individuals in the data disclosed by the government or prefectures. This is because latent individuals have not yet developed symptoms, making it difficult to observe them as latent individuals. In my SEIR model, as mentioned earlier, susceptible individuals are assumed to become infectious three days after infection. Therefore, in the data disclosed by the government or prefectures, it is assumed that the number of new infections corresponds to the first day of the latent period two days prior to symptom onset.

Furthermore, since we are interested only in individuals on the first day of the latent period ($E_{1.1}$), the formula for$E_{1.1}$is derived by subtracting the number of individuals on the first day of the latent period from the number of new infections disclosed daily, obtained by subtracting the number of individuals on the first day of the latent period from the number of new infections disclosed daily.

$$\frac{dE_{1.1}}{dt}(t) = \lambda_1(t) - E_{1.1}(t) \quad (6)$$

(7) coincides with the aforementioned content, yet designates individuals in Group 1 on the second day of the latent period as E1.2. Individuals on the first day of the latent period transition to those on the second day of the latent period the following day. Hence, subtracting the number of old second-day latent individuals from the number of new second-day latent individuals results in the count of second-day latent individuals on day t.

$$\frac{dE_{1.2}}{dt}(t) = E_{1.1}(t) - E_{1.2}(t) \quad (7)$$

(8) overlaps with the aforementioned information, designating individuals in Group 1 on the third day of the latent period as E1.3. Individuals on the second day of the latent period transition to those on the third day of the latent period the following day. Therefore, subtracting the number of old third-day latent individuals from the number of new third-day latent individuals results in the count of third-day latent individuals on day t.

$$\frac{dE_{1.3}}{dt}(t) = E_{1.2}(t) - E_{1.3}(t) \quad (8)$$

Let I_1 represent the infected individuals in Group 1. The infected individuals in Group 1 are those who were in the third day of the latent period the previous day. Additionally, among the infected individuals, there are those who recover from the infection and no longer remain infected. Those who have recovered from the infection are designated as recoveries (σ_1 or R_1). Infected individuals continue to accumulate as such until they recover from the infection.

$$\frac{dI_1}{dt}(t) = E_{1.3}(t-1) - \sigma_1 = I_1(t) - \sigma_1 \quad (9)$$

R_1 represents the daily number of recoveries in Group 1, where β denotes the recovery rate, and $I_1(t)$ represents the number of infected individuals. Multiplying these two yields the daily number of recoveries for Group 1. This is illustrated below.

$$\frac{dR_1}{dt}(t) = \sigma_1(t) \quad (10)$$

β represents the recovery rate, and $I_1(t)$ denotes the infected individuals. These two variables allow us to calculate the daily number of recoveries for Group 1. This is illustrated below.

$$\sigma_1(t) = \beta I_1(t) \quad (11)$$

The above elucidates equations (1) through (11) for Group 1. The equations for Groups 2, 3, and 4 involve merely substituting parameters such as initial values and coefficients with the values from Group 1, hence, explanation is omitted. The following is a list of

$$\frac{dS_1}{dt}(t) = -\lambda_1(t) \quad (4)$$

$$\frac{dE_{1.1}}{dt}(t) = \lambda_1(t) - E_{1.1}(t) \quad (6)$$

$$\frac{dE_{1.2}}{dt}(t) = E_{1.1}(t) - E_{1.2}(t) \quad (7)$$

$$\frac{dE_{1.3}}{dt}(t) = E_{1.2}(t) - E_{1.3}(t) \quad (8)$$

$$\frac{dI_1}{dt}(t) = E_{1.3}(t-1) - \sigma_1 = I_1(t) - \sigma_1 \quad (9)$$

$$\frac{dR_1}{dt}(t) = \sigma_1(t) \quad (10)$$

※ supplementation

$$\lambda_1^d = S_1^d(t)\frac{T_{1,1}}{N_1^d}\alpha_1\left(T_{1,1}E_1(t) + T_{2,1}E_2(t) + T_{3,1}E_3(t) + T_{4,1}E_4(t)\right)$$
$$+S_1^d(t)\frac{T_{1,2}}{N_2^d}\alpha_2\left(T_{1,2}E_1(t) + T_{2,2}E_2(t) + T_{3,2}E_3(t) + T_{4,2}E_4(t)\right)$$
$$+S_1^d(t)\frac{T_{1,3}}{N_3^d}\alpha_3\left(T_{1,3}E_1(t) + T_{2,3}E_2(t) + T_{3,3}E_3(t) + T_{4,3}E_4(t)\right)$$
$$+S_1^d(t)\frac{T_{1,4}}{N_4^d}\alpha_4\left(T_{1,4}E_1(t) + T_{2,4}E_2(t) + T_{3,4}E_3(t) + T_{4,4}E_4(t)\right) \quad (1)$$

$$\lambda_1^n = \alpha_1 h\frac{S_1^n(t)}{N_1^n}E_1(t) \quad (2)$$

$$\lambda_1(t) = \frac{1}{2}(\lambda_1^d + \lambda_1^n) \quad (3)$$

$$E_1(t) = E_{1.1}(t) + E_{1.2}(t) + E_{1.3}(t) \quad (5)$$

$$\sigma_1(t) = \beta I_1(t) \quad (11)$$

Figure 3: SEIR model for Group 1

$$\frac{dS_2}{dt}(t) = -\lambda_2(t) \quad (12)$$

$$\frac{dE_{2.1}}{dt}(t) = \lambda_2(t) - E_{2.1}(t) \quad (13)$$

$$\frac{dE_{2.2}}{dt}(t) = E_{2.1}(t) - E_{2.2}(t) \quad (14)$$

$$\frac{dE_{2.3}}{dt}(t) = E_{2.2}(t) - E_{2.3}(t) \quad (15)$$

$$\frac{dI_2}{dt}(t) = E_{2.3}(t-1) - \sigma_2 = I_2(t) - \sigma_2 \quad (16)$$

$$\frac{dR_2}{dt}(t) = \sigma_2(t) \quad (17)$$

※ supplementation

$$\lambda_2^d = S_2^d(t)\frac{T_{2,1}}{N_1^d}\alpha_1\left(T_{1,1}E_1(t) + T_{2,1}E_2(t) + T_{3,1}E_3(t) + T_{4,1}E_4(t)\right)$$
$$+S_2^d(t)\frac{T_{2,2}}{N_2^d}\alpha_2\left(T_{1,2}E_1(t) + T_{2,2}E_2(t) + T_{3,2}E_3(t) + T_{4,2}E_4(t)\right)$$
$$+S_2^d(t)\frac{T_{2,3}}{N_3^d}\alpha_3\left(T_{1,3}E_1(t) + T_{2,3}E_2(t) + T_{3,3}E_3(t) + T_{4,3}E_4(t)\right)$$
$$+S_2^d(t)\frac{T_{2,4}}{N_4^d}\alpha_4\left(T_{1,4}E_1(t) + T_{2,4}E_2(t) + T_{3,4}E_3(t) + T_{4,4}E_4(t)\right) \quad (18)$$

$$\lambda_2^n = \alpha_2 h\frac{S_2^n(t)}{N_2^n}E_2(t) \quad (19)$$

$$\lambda_2(t) = \frac{1}{2}(\lambda_2^d + \lambda_2^n) \quad (20)$$

$$E_2(t) = E_{2.1}(t) + E_{2.2}(t) + E_{2.3}(t) \quad (21)$$

$$\sigma_2(t) = \beta I_2(t) \quad (22)$$

Figure 4: SEIR model for Group 2

$$\frac{dS_3}{dt}(t) = -\lambda_3(t) \quad (23)$$

$$\frac{dE_{3.1}}{dt}(t) = \lambda_3(t) - E_{3.1}(t) \quad (24)$$

$$\frac{dE_{3.2}}{dt}(t) = E_{3.1}(t) - E_{3.2}(t) \quad (25)$$

$$\frac{dE_{3.3}}{dt}(t) = E_{3.2}(t) - E_{3.3}(t) \quad (26)$$

$$\frac{dI_3}{dt}(t) = E_{3.3}(t-1) - \sigma_3 = I_3(t) - \sigma_3 \quad (27)$$

$$\frac{dR_3}{dt}(t) = \sigma_3(t) \quad (28)$$

※ supplementation

$$\lambda_3^d = S_3^d(t)\frac{T_{3,1}}{N_1^d}\alpha_1\left(T_{1,1}E_1(t) + T_{2,1}E_2(t) + T_{3,1}E_3(t) + T_{4,1}E_4(t)\right)$$
$$+S_3^d(t)\frac{T_{3,2}}{N_2^d}\alpha_2\left(T_{1,2}E_1(t) + T_{2,2}E_2(t) + T_{3,2}E_3(t) + T_{4,2}E_4(t)\right)$$
$$+S_3^d(t)\frac{T_{3,3}}{N_3^d}\alpha_3\left(T_{1,3}E_1(t) + T_{2,3}E_2(t) + T_{3,3}E_3(t) + T_{4,3}E_4(t)\right)$$
$$+S_2^d(t)\frac{T_{3,4}}{N_4^d}\alpha_4\left(T_{1,4}E_1(t) + T_{2,4}E_2(t) + T_{3,4}E_3(t) + T_{4,4}E_4(t)\right) \quad (29)$$

$$\lambda_3^n = \alpha_3 h\frac{S_3^n(t)}{N_3^n}E_3(t) \quad (30)$$

$$\lambda_3(t) = \frac{1}{2}(\lambda_3^d + \lambda_3^n) \quad (31)$$

$$E_3(t) = E_{3.1}(t) + E_{3.2}(t) + E_{3.3}(t) \quad (32)$$

$$\sigma_3(t) = \beta I_3(t) \quad (33)$$

Figure 5: SEIR model for Group 3

$$\frac{dS_4}{dt}(t) = -\lambda_4(t) \quad (34)$$

$$\frac{dE_{4.1}}{dt}(t) = \lambda_4(t) - E_{4.1}(t) \quad (35)$$

$$\frac{dE_{4.2}}{dt}(t) = E_{4.1}(t) - E_{4.2}(t) \quad (36)$$

$$\frac{dE_{4.3}}{dt}(t) = E_{4.2}(t) - E_{4.3}(t) \quad (37)$$

$$\frac{dI_4}{dt}(t) = E_{4.3}(t-1) - \sigma_4 = I_4(t) - \sigma_4 \quad (38)$$

$$\frac{dR_4}{dt}(t) = \sigma_4(t) \quad (39)$$

※ supplementation

$$\lambda_4^d = S_4^d(t)\frac{T_{4,1}}{N_1^d}\alpha_1\left(T_{1,1}E_1(t) + T_{2,1}E_2(t) + T_{3,1}E_3(t) + T_{4,1}E_4(t)\right)$$
$$+S_4^d(t)\frac{T_{4,2}}{N_2^d}\alpha_2\left(T_{1,2}E_1(t) + T_{2,2}E_2(t) + T_{3,2}E_3(t) + T_{4,2}E_4(t)\right)$$
$$+S_4^d(t)\frac{T_{4,3}}{N_3^d}\alpha_3\left(T_{1,3}E_1(t) + T_{2,3}E_2(t) + T_{3,3}E_3(t) + T_{4,3}E_4(t)\right)$$
$$+S_4^d(t)\frac{T_{4,4}}{N_4^d}\alpha_4\left(T_{1,4}E_1(t) + T_{2,4}E_2(t) + T_{3,4}E_3(t) + T_{4,4}E_4(t)\right) \quad (40)$$

$$\lambda_4^n = \alpha_4 h\frac{S_4^n(t)}{N_4^n}E_4(t) \quad (41)$$

$$\lambda_4(t) = \frac{1}{2}(\lambda_4^d + \lambda_4^n) \quad (42)$$

$$E_4(t) = E_{4.1}(t) + E_{4.2}(t) + E_{4.3}(t) \quad (43)$$

$$\sigma_4(t) = \beta I_4(t) \quad (44)$$

Figure 6: SEIR model for Group 4

3 Methods

This section provides a clear and detailed explanation of the parameter estimation process used in the study, including the sources of data, the calculation of specific parameters, and the tools and techniques used for the experiments and numerical computations

In estimating parameters such as initial values, data from various sources were utilized, including the publicly available data from the National Institute of Infectious Diseases (4), population and daytime mobility data from Saitama, Tokyo, Kanagawa, and Chiba prefectures (5), and newly infected data from Saitama, Tokyo, Kanagawa, and Chiba prefectures (6). These data were used to determine coefficients such as infection rate, recovery rate, and mobility rate. This study employed numerical data regarding nationwide infections from January 3, 2022, to April 10, 2022. This period was chosen because the COVID-19 outbreak during this time was attributed to the BA.1 lineage of the Omicron variant, and the BA.2 lineage, with different characteristics, was expected to emerge after this date. Different variants of COVID-19 may have varying infection rates, recovery rates, and latent periods, even

though they are all referred to as COVID-19. Therefore, this study focuses on the BA.1 lineage of the Omicron variant, which surged from the first to the fourteenth week of 2022.

Table 1: Parameters such as infection rates

character	meaning	numerical value
$\alpha 1$	Group 1 infection rate	0.213
$\alpha 2$	Group 2 infection rate	0.149
$\alpha 3$	Group 3 infection rate	0.168
$\alpha 4$	Group 4 infection rate	0.145
$T_{1.1}$	of those who stay in group 1	0.967
$T_{1.2}$	Movement rate from Group 1 to Group 2	0.01
$T_{1.3}$	Movement rate from Group 1 to Group 3	0.006
$T_{1.4}$	Movement rate from Group 1 to Group 4	0.017
$T_{2.1}$	Movement rate from Group 2 to Group 1	0.148
$T_{2.2}$	of those who stay in group 2	0.842
$T_{2.3}$	Movement rate from Group 2 to Group 3	0.004
$T_{2.4}$	Movement rate from Group 2 to Group 4	0.006
$T_{3.1}$	Movement rate from Group 3 to Group 1	0.118
$T_{3.2}$	Movement rate from Group 3 to Group 2	0.001
$T_{3.3}$	of those who stay in group 3	0.879
$T_{3.4}$	Movement rate from Group 3 to Group 4	0.002
$T_{4.1}$	Movement rate from Group 4 to Group 1	0.143
$T_{4.2}$	Movement rate from Group 4 to Group 2	0.008
$T_{4.3}$	Movement rate from Group 4 to Group 3	0.845
$T_{4.4}$	of those who stay in group 4	0.004
h	Prevalence of secondary infections within cohabiting families	0.35
β	recovery rate	0.1

The parameters mentioned above are computed as follows. Initially, the daily new infection numbers for Saitama, Tokyo, Kanagawa, and Chiba prefectures are compiled in Excel, and the average of these new infection numbers is determined. Subsequently, the differential equations of the SEIR model are rearranged such that only the infection rate remains on the left-hand side. By substituting the actual data from Tokyo for Group 1, Saitama for Group 2, Kanagawa for Group 3, and Chiba for Group 4, α_1, α_2, α_3, and α_4 are calculated.

The determination of the mobility rate T is based on data on the population and daytime mobility from Saitama, Tokyo, Kanagawa, and Chiba prefectures.

The secondary infection rate within households h is referenced from the announcement data

of the National Institute of Infectious Diseases.

Regarding the recovery rate β, considering the Omicron variant prevalent around January, the recovery period was estimated to be 10 days. Assuming symptoms resolve definitively 10 days after onset, the daily recovery rate is set at 0.1(7).

Experiments were performed using Python. RK45 was used to solve the simultaneous differential equations.

4 Results

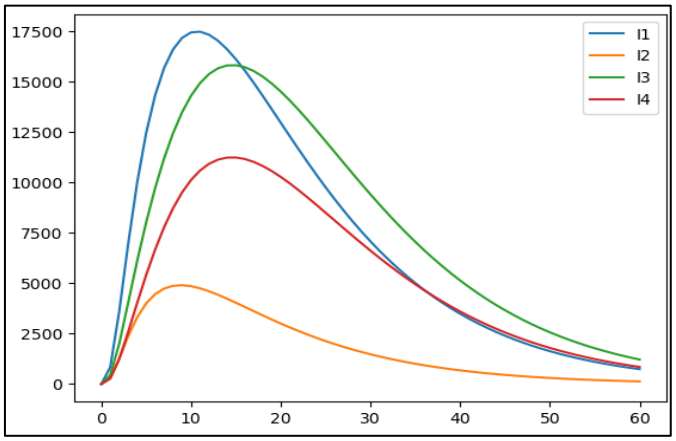

Figure 7: Simulation Results

This section provides a concise and clear presentation of the key findings of the simulations, comparing them with real-world data and highlighting the impact of variations in mobility on the total peak number of new infections between groups.

IIn the simulation results, the number of new infections and the total number of latent individuals exhibited outcomes similar to those depicted in Figure 7 above. The peak number of new infections in Group 1 reached 17,486 individuals on the 9th day since the start of the simulation. For Group 2, the peak number of new infections was 4,907 individuals on the 11th day since the start of the simulation. In the case of Group 3, the peak number of new infections occurred on the 15th day since the start of the simulation, with 15,821 individuals affected. Similarly, for Group 4, the highest number of new infections, reaching 11,242 individuals, was observed on the 15th day since the start of the simulation.

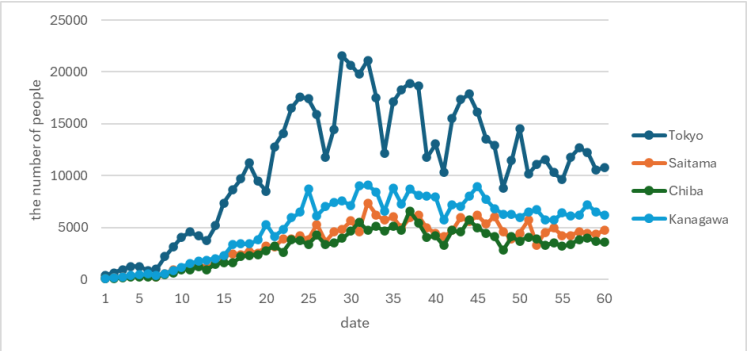

Figure 8: Data on the number of new infections in the referenced prefectures

From January 5th to March 5th, the highest number of new infections occurred on the 32nd day in Tokyo, with 21,110 individuals affected, followed by Saitama Prefecture with 7,353 individuals on the same day, Chiba Prefecture with 6,599 individuals on the 37th day, and Kanagawa Prefecture with 9,096 individuals on the 32nd day.

Table 2: Simulation results with varying mobility rates

character	numerical value			
$T_{1.1}$	1	0.25	0.7	0.1
$T_{1.2}$	0	0.25	0.1	0.3
$T_{1.3}$	0	0.25	0.1	0.3
$T_{1.4}$	0	0.25	0.1	0.3
$T_{2.1}$	0	0.25	0.1	0.3
$T_{2.2}$	1	0.25	0.7	0.1
$T_{2.3}$	0	0.25	0.1	0.3
$T_{2.4}$	0	0.25	0.1	0.3
$T_{3.1}$	0	0.25	0.1	0.3
$T_{3.2}$	0	0.25	0.1	0.3
$T_{3.3}$	1	0.25	0.7	0.1
$T_{3.4}$	0	0.25	0.1	0.3
$T_{4.1}$	0	0.25	0.1	0.3
$T_{4.2}$	0	0.25	0.1	0.3
$T_{4.3}$	0	0.25	0.1	0.3
$T_{4.4}$	1	0.25	0.7	0.1
Highest number of new infections				
Group1	16204.63	18458.88	16410.08	20061.35
Group2	4646.433	8576.16	6828.08	8776.14
Group3	10962.05	9963.21	10873.76	9612.22
Group4	7266.41	7985.38	8581.73	7488.35
Total Peak Number of New Infections from Group 1 to Group 4				
	38799.29	44945.8	42553.56	45925.33

Table 2 presents simulation results with variations in mobility across four patterns. When inter-group movement is the most frequent, the total peak number of new infections between each group is highest, whereas scenarios with no movement exhibited the lowest total peak number of new infections between groups.

5 Discussion

The simulation results did not closely resemble the trends observed in real-world data. In all scenarios, the peaks occurred earlier and the outbreak subsided more rapidly than in actual data. The peak number of new infections in each group ranged from approximately 8 to 15 days in the simulations, resulting in a difference of around 3,000 individuals in the peak number of new infections compared to actual data. Moreover, each simulation recorded the peak number of new infections earlier than the real-world data. Subsequently, the number of recoveries surpassed the number of infections, and the outbreak appeared to gradually subside.

The earlier peak observed in the simulation results compared to real-world data may be attributed to factors such as the lack of incorporation of immunity acquisition through vaccination in the model, leading to a rapid spread of the infection in the simulations. Furthermore, the differences in the peak number of new infections may be attributed to the consideration of movement only between the four groups, as well as the extreme division of movement into daytime activity and nighttime confinement. In reality, individuals from prefectures other than Saitama, Kanagawa, and Chiba may also move to Tokyo, and people may also travel from overseas. Additionally, variations in infection rates based on location are also conceivable. For example, outdoor sidewalks, office spaces, bars, and clubs are unlikely to all have the same infection rate. The oversight in considering these factors may have resulted in discrepancies between the simulation results and the real-world data.

Furthermore, when examining the data with varying mobility rates, Table 2 reveals that moving to groups with higher infection rates resulted in approximately 1.18 times more new infections compared to when no movement occurred. Measures such as remote work and online classes have been implemented to prevent the spread of infection during the COVID-19 pandemic. Refraining from unnecessary outings has significantly contributed to infection prevention.

6 Conclusion

In order to address two questions regarding the extent of the impact of human mobility on infection outbreaks and the estimation of the number of latent individuals, a simulation of the SEIR model was conducted, taking into account changes in contact rates due to daytime and nighttime mobility. To make the settings more realistic, data from the National Institute of Infectious Diseases (4), daytime mobility data for residents of Saitama, Tokyo, Kanagawa, and Chiba (5), as well as publicly available data on new infections in Saitama, Tokyo, Kanagawa, and Chiba prefectures (6), were used to determine initial values between groups and calculate parameters by substituting them into the differential equations of the SEIR model.

The simulation results were somewhat divergent from real-world data. Additionally, when the inter-group mobility rates were altered in subsequent simulations, a difference of approximately 1.18 times in peak new infections was observed between scenarios where individuals from low infection rate groups did not move to high infection rate groups and scenarios where they did move. This suggests that human mobility could be a contributing factor to infection spread. Therefore, it can be argued that measures such as online classes and remote work, which reduce human mobility, can help mitigate the spread of infection during outbreaks.

It should be noted that factors such as mobility of individuals outside the four groups,

immunity acquisition through vaccination, the possibility of reinfection due to immunity acquired after infection, and population changes due to births and deaths and healthcare system collapse due to infection spread were not considered in this study. Creating a new model that takes these factors into account and conducting simulations closer to real-world trends is a future challenge.

Acknowledgement

This work was partly supported by Grant-in-Aid for Scientific Research (C) No. 22K02815 and No.23K02697 from the Japan Society for the Promotion of Science (JSPS).

References

[1] W. O. Kermack and A. G. McKendrick, Contributions to the mathematical theory of epidemics-I, Proceedings of the Royal Society, 1927, 115A: 700-721

[2] H. Inaba, Mathematical Models of Infectious Diseases, bafukan,2022

[3] R. Sakamaki, S. Fujita, SIR Model with the Person Trip to Analyze the Epidemic of Influenza, Proceedings of the 7th IIAE International Conference on Intelligent Systems and Image Processing, 2019

[4] National Institute of Infectious Diseases, "Transition of Secondary Infection Rate by Period of Variant Strain Epidemic in COVID-19", https://www.niid.go.jp/niid/ja/2019-ncov/2502-idsc/iasr-in/11636-513c03.html, Accessed 1/10/2024.

[5] e-stat, Japan in Statistics, https://www.e-stat.go.jp/stat-search/files?page=1&layout=datalist&toukei=00200521&tstat=000001136464&cycle=0&tclass1=000001136469&result_page=1&tclass2val=0, 4/10/2024.

[6] Ministry of Health, Labour and Welfare, Open Data, https://www.mhlw.go.jp/stf/covid-19/open-data.html, 4/14/2024.

[7] Ministry of Health, Labour and Welfare, Revision of Discharge Criteria and Removal Criteria, https://www.mhlw.go.jp/content/000639696.pdf, 12/28/2023.